Journal of Physics B: Atomic, Molecular and Optical Physics

PAPER

Single- and multiple-electron processes in water molecules colliding with proton beams

To cite this article: P N Terekhin *et al* 2018 *J. Phys. B: At. Mol. Opt. Phys.* **51** 235201

View the article online for updates and enhancements.

IOP ebooks™

Bringing you innovative digital publishing with leading voices to create your essential collection of books in STEM research.

Start exploring the collection - download the first chapter of every title for free.

This content was downloaded from IP address 168.96.15.8 on 12/11/2018 at 16:27

IOP Publishing Journal of Physics B: Atomic, Molecular and Optical Physics
J. Phys. B: At. Mol. Opt. Phys. **51** (2018) 235201 (9pp) https://doi.org/10.1088/1361-6455/aadb22

Single- and multiple-electron processes in water molecules colliding with proton beams

P N Terekhin[1,2,4], **M A Quinto**[1], **J M Monti**[1,3], **O A Fojón**[1,3] and **R D Rivarola**[1,3]

[1] Instituto de Física Rosario (CONICET-UNR), Bv 27 de Febrero 210 bis, 2000 Rosario, Argentina
[2] National Research Centre 'Kurchatov Institute', Kurchatov Sq. 1, 123182 Moscow, Russia
[3] Laboratorio de Colisiones Atómicas, Facultad de Ciencias Exactas, Ingeniería y Agrimensura, Universidad Nacional de Rosario, Av. Pellegrini 250, 2000 Rosario, Argentina

E-mail: p.n.terekhin@yandex.ru

Received 11 May 2018, revised 27 July 2018
Accepted for publication 17 August 2018
Published 6 November 2018

Abstract

Single- and multiple-electron removal processes (ionization, capture and transfer-ionization) from water molecules by the impact of protons have been studied. A prior version of the three-body continuum distorted wave-eikonal initial state (3B-CDW-EIS) approximation within the independent electron approximation is used to calculate transition probabilities as a function of the impact parameter and consequently pure and net absolute cross sections for the collisions under consideration. A unitarization procedure is employed to avoid possible overestimation of the 3B-CDW-EIS single-particle impact parameter probabilities at intermediate collision energies. Multiple-electron transitions are determined using a statistical multinomial distribution. A critical analysis of the validity of this type of distribution for describing pure single-electron processes is presented. The results are compared with other theoretical calculations and available experimental data at impact energies from 50 keV to 5 MeV. New physical insights into the reactions studied are introduced.

Keywords: water, multiple-electron processes, ion–molecule collisions, electron ionization, electron capture, transfer-ionization

(Some figures may appear in colour only in the online journal)

1. Introduction

The interaction of charged particles with molecular targets is of fundamental interest in current research areas such as plasma physics [1], thermonuclear fusion [2] and others. In particular, collisions between fully stripped ions and water (H_2O) receive much attention in biology and medicine [3]. Irradiation of biological matter by ion beams produces secondary species (such as electrons, ions and radicals) along the radiation track, which can further react within irradiated cells to provoke critical DNA lesions such as base damages and single- or double-strand breaks, and then induce radiation effects such as the arrest of cell division, chromosomal aberrations, mutation and cell-death [4, 5]. Indeed, DNA lesions and, more particularly, those involved in clustered damages are considered of prime importance for describing post-irradiation cellular survival [6].

Under these conditions, improved theoretical models, as well as experimental data, of ion-induced collisions on DNA remain crucial nowadays. As a first step, investigation of single- and multiple-electron removal processes occurring between fully stripped ions and H_2O molecules is of fundamental interest. It is well known that secondary electrons play an important role in radiation-induced biological effects. A large number of electrons can be produced in the Bragg peak region in a collision with fast charged particles, where incident ions lose most of their kinetic energy. These electrons may induce ionization and fragmentation of neighboring molecules.

[4] Present address: Department of Physics and Research Center OPTIMAS, Technical University of Kaiserslautern, Erwin-Schrödinger-Straße 46, 67663 Kaiserslautern, Germany.

 © 2018 IOP Publishing Ltd Printed in the UK

The large amount of interest in this issue has led to the formulation of various theoretical models. To calculate differential cross sections and total cross sections (TCSs) for the ionization of H_2O molecules, a number of semi-empirical methods have been applied [7–10]. Also, descriptions based on the Born approximation [11–14] and on different versions of the various continuum distorted wave-eikonal initial state models [9, 15–17] have been considered to describe the ionization or capture reactions resulting from the collision of heavy ions with H_2O-vapor targets. Investigations of multiple ionization, capture and transfer-ionization processes for ion$-H_2O$ systems have also been performed in the framework of the nonperturbative basis generator method (BGM) [18] and using the classical trajectory Monte Carlo (CTMC) treatment [19–22].

A large variety of final projectile and target charge states may be produced during the collision processes. Consequently, calculations of cross sections of pure ionization, capture and transfer-ionization reactions are essential in order to determine the main features of multiple-electron processes.

In the BGM, single-electron removal probabilities from each molecular orbital (MO) are investigated through an *inclusive* probability formalism. A single-particle model is employed, where a set of oxygen atomic orbitals (AOs) obtained from density functional theory calculations and hydrogenic projectile states together with 22 pseudo-states are included to describe the MOs and ionization channels [23].

In a previous work [17], a molecular version of the continuum distorted wave-eikonal initial state model (CDW-EIS-MO) within a three-body description (active electron, residual target and projectile) was employed. The MOs were constructed as contractions of Gaussian-type functions, using the STO-3G basis set [24] based on a Hartree–Fock approach, and the associated orbital energies were determined. A CNDO (complete neglect of the differential overlap) description of the MOs, obtained as a weighted sum of atomic probabilities corresponding to the molecule compounds, was also employed. Using an independent particle approximation, net and pure cross sections were calculated for ionization by the impact of proton beams using a binomial statistical distribution which does not take into account the influence of electron capture probabilities. Its inclusion may play a principal role at intermediate collision velocities. Net electron capture cross sections were also reported. It was shown that cross sections obtained by using the more complex Hartree–Fock wave functions or the CNDO representation of the MOs give negligible differences, for both electron capture and ionization processes.

An alternative three-body CDW-EIS model (3B-CDW-EIS) [25–29] is used in the present work in order to calculate transition probabilities (capture and ionization) as a function of the impact parameter and absolute cross sections for the considered collisions. Our main scope is the investigation of *pure* electron processes where the active electron is ionized (and/or captured) while the residual electrons are considered frozen: they remain in their initial orbitals during the collision. With this aim in mind, for multiple-electron reactions, we use a statistical multinomial distribution within the independent electron approximation instead of a binomial one, where the influence of electron capture on ionization, and vice versa, is included in the treatment. For simplicity, and following the above described results, the initial wave functions of the active electrons bound to a particular H_2O MO are described by means of the CNDO approximation [30]. Roothaan–Hartree–Fock (RHF) wave functions [31] are employed to represent the states of the atomic compounds of the MOs. We must note that in recent work on the single-electron ionization (SI) of H_2O molecules by multiple charged ions, where double differential cross sections (DDCSs) were calculated using a molecular representation of the target [32] or a CNDO approximation of the orbitals, only minor differences were obtained [16]. The origin of this agreement could come from the fact that when the molecular description is used to calculate DDCSs an average over all molecular orientations is necessary. Cross sections, however, are very sensitive to the orbital energies employed in the calculations [33]. Thus, we use the orbital energies obtained with a more complete 3-21G basis set [34]. We consider Coulombic continuum wave functions for each one of the MOs with effective charges obtained from their corresponding binding energies. This description has been used with success to describe DDCSs [16, 35, 36]. Also, in the BGM and CDW-EIS-MO models, only the four valence orbitals were considered, which appears to be sufficient when TCSs are calculated. However, in [16] it was shown that the deepest $1a_1$ orbital dominates the DDCS for large electron velocities at forward and backwards emission angles. So, we prefer to consider all the MOs of H_2O vapor. Furthermore, as in the BGM and CDW-EIS-MO models, transitions to excited states of the molecule are here neglected.

As probabilities may give values larger than unity at intermediate collision energies, even for proton projectiles, we employ the Sidorovich unitarization procedure [37], which has been applied with success, and playing a crucial role, to describe DDCSs within the CDW-EIS approximation, for the impact of Au^{53+} on Ar and Ne atoms [38]. This approximation corresponds to the solution of differential balance equations for the populations of the final states provided that inverse transitions to the initial state are neglected. On the experimental side, a significant number of measurements have been performed especially for pure reactions in proton$-H_2O$ collisions [10, 39–44], with the consideration that they may offer more detailed physical information on the reactions studied.

The paper is organized as follows. The 3B-CDW-EIS formalism for a proton$-H_2O$ collision is introduced in section 2. The results and discussion for single and multiple ionization reactions are presented in section 3.1, for single-electron capture (SC) and transfer-ionization in section 3.2 and for net ionization and capture in section 3.3. Conclusions are given in section 4.

Atomic units are used throughout the paper unless otherwise stated.

2. Theoretical model

In this work we investigate the collision of a bare nucleus with charge Z_P and a molecular target. For the impact energies considered here (50 keV to 5 MeV) the interaction process is sufficiently fast that we can neglect rotational and vibrational degrees of freedom of the target and we consider that the target position is spatially fixed during the reaction.

In order to reduce the multielectronic problem to a three-body one, we assume that there is only one active electron whereas the rest (passive) ones remain frozen in their initial orbitals during the collision. Thus, the residual target acts as a core and the two other bodies are the projectile and the active electron. This approximation has previously been applied with success (see for example reference [25]). Using the straight-line version of the impact parameter approximation, where $\mathbf{R} = \boldsymbol{\rho} + \mathbf{v}t$ is the internuclear vector, $\boldsymbol{\rho}$ is the impact parameter vector, $\mathbf{v}$ is the projectile velocity parallel to the z-axis of the laboratory reference frame with origin fixed in the center of mass of the target and t is the evolution time, the single-electron Hamiltonian can be written in the form

$$H = -\frac{\nabla^2}{2} - \frac{Z_P}{\mathbf{s}} - \sum_i \frac{Z_{T_i}}{x_i} + V_{ap}(\mathbf{r}) + V_S(\mathbf{R}), \tag{1}$$

where $\mathbf{s}$ represents the active-electron position vector with respect to the projectile ion, the sum takes into account interactions of the active electron with all the molecular nuclei with nuclear charges Z_{T_i}, and x_i is the position of the active electron with respect to the ith target nucleus. The term $V_{ap}(\mathbf{r})$ in equation (1) describes the interaction between the active electron and the passive ones

$$V_{ap}(\mathbf{r}) = \langle \varphi_p(\{\mathbf{r}_{pj}\}) \left| \sum_{j=1}^{N_p} \frac{1}{|\mathbf{r} - \mathbf{r}_{pj}|} \right| \varphi_p(\{\mathbf{r}_{pj}\})\rangle, \tag{2}$$

with $\mathbf{r}$ being the active-electron position vector with respect to the laboratory reference frame, $\varphi_p(\{\mathbf{r}_{pj}\})$ is the wave function which corresponds to the N_p passive electrons and $\{\mathbf{r}_{pj}\}$ indicates the ensemble of position vectors of the jth passive electrons. The last term in equation (1), $V_S(\mathbf{R})$, is the static potential which corresponds to the residual target−projectile interaction. As it is independent of the active-electron coordinates, it is relevant only for the projectile angular distribution and it cannot generate electronic transitions. So, it will be neglected hereafter [25].

The transition amplitude for SI or SC can be written as

$$\mathrm{A}_{if}^{ion,cap}(\boldsymbol{\rho}, \mathbf{k}) = -i \int_{-\infty}^{+\infty} dt \langle \chi_f^{ion,\,cap} | \left(H - i\frac{\partial}{\partial t} \right) | \chi_i \rangle, \tag{3}$$

where it is assumed that

$$\lim_{t \to +\infty} \langle \chi_f^{ion,cap} | \chi_i \rangle = 0. \tag{4}$$

In equation (3), $\mathbf{k}$ is the linear momentum of the ejected electron. The initial χ_i and final $\chi_f^{ion,cap}$ wave functions for ionization and capture, respectively, are chosen as

$$\chi_i = \Phi_i(\mathbf{r}, t) L_i^{EIS}(\mathbf{s}), \tag{5}$$

$$\chi_f^{ion} = \Phi_f^{ion}(\mathbf{r}, t) L_f^{CDW,ion}(\mathbf{s}), \tag{6}$$

$$\chi_f^{cap} = \Phi_f^{cap}(\mathbf{s}, t) L_f^{CDW,cap}(\mathbf{r}), \tag{7}$$

where

$$\Phi_i(\mathbf{r}, t) = \varphi_i(\mathbf{r}) \exp(-i\varepsilon_i t), \tag{8}$$

$$\begin{aligned} \Phi_f^{ion}(\mathbf{r}, t) &= \varphi_k(\mathbf{r}) \exp(-i\varepsilon_f^{ion} t) \\ &= (2\pi)^{-3/2} \exp(-i\varepsilon_f^{ion} t + i\mathbf{kr}) N^*(\xi) {}_1\mathrm{F}_1 \\ &\quad \times (-i\xi;\, 1;\, -ikr - i\mathbf{kr}), \end{aligned} \tag{9}$$

$$\Phi_f^{cap}(\mathbf{s}, t) = \varphi_f(\mathbf{s}) \exp\left(-i\varepsilon_f^{cap} t + i\mathbf{vr} - i\frac{v^2}{2} t \right), \tag{10}$$

with φ_i being the initial bound orbital of the active electron of the H_2O molecule. The MOs are described employing the CNDO approximation [30], φ_k is the continuum wavefunction of the active electron, φ_f is the final-state bound wavefunction, $\varepsilon_f^{ion} = k^2/2$ is the final ejected-electron energy, and ε_f^{cap} is the orbital energy of the captured electron. The distortion factors, associated with the active-electron−projectile interaction, are given by

$$L_i^{EIS}(\mathbf{s}) = \exp[-iv \ln(vs + \mathbf{vs})], \tag{11}$$

$$L_f^{CDW,ion}(\mathbf{s}) = N^*(\zeta) {}_1\mathrm{F}_1(-i\zeta;\, 1;\, -ips - i\mathbf{ps}), \tag{12}$$

$$L_f^{CDW,cap}(\mathbf{r}) = N^*(\xi) {}_1\mathrm{F}_1(-i\xi;\, 1;\, -ivr - i\mathbf{vr}), \tag{13}$$

where $v = Z_p/v$, $\zeta = Z_p/p$ with $\mathbf{p} = \mathbf{k} - \mathbf{v}$ the linear momentum of the ejected electron with respect to the projectile, $N(a) = \exp(\pi a/2)\Gamma(1 + ia)$ with Γ the Gamma function and ${}_1\mathrm{F}_1(a;1;b)$ the Kummer confluent hypergeometric function. Also $\xi = Z_T^*/k$, where an effective charge Z_T^* was introduced in order to replace the active-electron−residual-target interaction by an effective Coulombic one, defined by the equation:

$$V_T(\mathbf{r}) = \sum_i \frac{(-Z_{T_i})}{x_i} + V_{ap}(\mathbf{r}) \simeq -\frac{Z_T^*}{r}. \tag{14}$$

The single-active-electron ionization probability, differential in the final electron energy E_k and solid angle Ω_k subtended by the ejected electron, is defined as

$$\frac{d^3 p^{ion}(\rho, \mathbf{k})}{dE_k d\Omega_k} = \frac{k}{2\pi} \int_0^{2\pi} d\varphi_\rho |A_{if}^{ion}(\boldsymbol{\rho}, \mathbf{k})|^2. \tag{15}$$

The full SI probability is obtained by integration of equation (15) over E_k and Ω_k:

$$p^{ion}(\rho) = \iint dE_k d\Omega_k \frac{d^3 p^{ion}(\rho, \mathbf{k})}{dE_k d\Omega_k}. \tag{16}$$

For electron capture the single-particle probability is given by

$$p^{cap}(\rho) = \frac{1}{2\pi} \int_0^{2\pi} d\varphi_\rho |A_{if}^{cap}(\boldsymbol{\rho})|^2, \tag{17}$$

where the integration in equations (15) and (17) is performed over the azimuthal angle φ_ρ of the impact parameter vector. We refer to $p^{ion,cap}$ as the probability of a single electron being removed from a given orbital.

A_{if} is computed from the matrix element R_{if}, which is given as a function of transverse momentum transfer $\boldsymbol{\eta}$, by applying the Fourier transform, as follows:

$$A_{if}^{ion,cap}(\boldsymbol{\rho}) = \frac{1}{2\pi}\int d\boldsymbol{\eta} e^{-i\boldsymbol{\eta}\boldsymbol{\rho}} R_{if}^{ion,cap}(\boldsymbol{\eta}). \tag{18}$$

The expression for $R_{if}^{ion,cap}$ has been previously reported in [27] and [29] for ionization and capture, respectively.

The ground state of H_2O is described by the known configuration $(1a_1)^2(2a_1)^2(1b_2)^2(3a_1)^2(1b_1)^2$. The probabilities of ionization and capture for a particular MO can be calculated as a linear combination of those corresponding to the AOs that compound the given MO. Based on the population analysis arising from the CNDO approach [16], the probabilities of each H_2O MO are given by:

$$\tilde{p}_{1a_1}^{ion,cap} = 2p_{O_{1s}(1a_1)}^{ion,cap}, \tag{19}$$

$$\tilde{p}_{2a_1}^{ion,cap} = 1.48p_{O_{2s}(2a_1)}^{ion,cap} + 0.52p_{H_{1s}(2a_1)}^{ion,cap}, \tag{20}$$

$$\tilde{p}_{1b_2}^{ion,cap} = 1.18p_{O_{2p}(1b_2)}^{ion,cap} + 0.82p_{H_{1s}(1b_2)}^{ion,cap}, \tag{21}$$

$$\tilde{p}_{3a_1}^{ion,cap} = 0.22p_{O_{2s}(3a_1)}^{ion,cap} + 1.44p_{O_{2p}(3a_1)}^{ion,cap} + 0.34p_{H_{1s}(3a_1)}^{ion,cap}, \tag{22}$$

$$\tilde{p}_{1b_1}^{ion,cap} = 2p_{O_{2p}(1b_1)}^{ion,cap}. \tag{23}$$

The corresponding MO energies are: $\varepsilon_{1a_1} = -19.842$ au, $\varepsilon_{2a_1} = -1.18$ au, $\varepsilon_{1b_2} = -0.67$ au, $\varepsilon_{3a_1} = -0.54$ au, $\varepsilon_{1b_1} = -0.46$ au. The effective charge Z_T^* in equation (14) is chosen as $Z_T^* = \sqrt{-2n_i^2\varepsilon_i}$ [45], where n_i is the principal quantum number of each atomic compound of the molecule and ε_i is the active-electron binding energy of a given MO. The SI and SC probabilities are defined as $p_j^{ion,cap} = \tilde{p}_j^{ion,cap}/2$, where $j \in \{1a_1, 2a_1, 1b_2, 3a_1, 1b_1\}$, because each MO is populated by two electrons. Thus, the $p_j^{ion,cap}$ describes the probability of a single-electron removal (ionization or capture) from a given jth MO. We average the probabilities of ionization and capture from the 2p subshell of the oxygen atom as

$$p_{2p}^{ion,cap} = \frac{p_{2p_0}^{ion,cap} + 2p_{2p_1}^{ion,cap}}{3}. \tag{24}$$

The electron capture probabilities are calculated as

$$p^{cap} = \sum_{n=1}^{3} p_n^{cap}, \tag{25}$$

where n is the principal quantum number corresponding to the different projectile excited states [29].

Taking into account the fact that SC or SI are represented by employing the model introduced above, where the passive electrons must remain frozen during the collision and so cannot be promoted to other states, we may conclude that the corresponding probabilities may have an exclusive character.

We describe in the following the case where various electrons are removed from the target. Considering the difficulties of using a multielectronic representation, we decided to employ a statistical multinomial analysis [46] based on the independent particle approximation. Considering that for single-electron reactions we have assumed a 'one-active-electron model', where this electron evolves throughout the entire collision time independently of the other electrons, which remain frozen and bound to the residual target, we adopt this image for multiple-electron processes. This means that in the multiple reaction each one of the 'active' electrons evolves in a similar, independent way. Thus, the probability for q-order ionization or q-order capture is given by the expression:

$$P_q^{ion,cap} = \sum_{q_1,\ldots,q_m=0}^{N_1,\ldots,N_m} \delta_{q,\sum_j q_j} \prod_{j=1}^{m} \binom{N_j}{q_j} (p_j^{ion,cap})^{q_j} \cdot (1 - p_j^{ion,cap} - p_j^{cap,ion})^{N_j - q_j}, \quad q \geqslant 2, \tag{26}$$

where m is the total number of MOs of the target, N_j is the number of electrons in the jth MO before the collision, q_j is the number of electrons removed from the jth MO and the Kronecker δ selects those combinations of electrons ionized (captured) from the active MO. In [17] a binomial distribution for q-order ionization was used. It is equivalent to neglecting the third term p_j^{cap} contained in the parenthesis of equation (26), and thus to disregarding the influence of electron capture on electron ionization. Moreover, charge exchange probabilities were obtained in [17] in an approximated way by the continuation of SI probabilitites just below the ionization threshold.

TCSs for q-order ionization/capture can be expressed as

$$\sigma_q^{ion,cap} = 2\pi \int \rho P_q^{ion,cap}(\rho) d\rho, \tag{27}$$

where $P_q^{ion,cap}(\rho)$ is hereafter calculated using the three-body approximation given by equations (16) and (25) but adding the contributions from all MOs.

TCSs of multiple-transfer processes for the ionization of k electrons to the continuum with simultaneous capture of l electrons are calculated using the expression:

$$P_{k,l}^{tot} = \sum_{k_1,\ldots,k_m=0}^{N_1,\ldots,N_m} \sum_{l_1,\ldots,l_m=0}^{N_1,\ldots,N_m} \delta_{k,\sum_j k_j} \delta_{l,\sum_j l_j} \prod_{j=1}^{m} \binom{N_j}{k_j + l_j} \binom{k_j + l_j}{k_j} \cdot (p_j^{ion})^{k_j} \cdot (p_j^{cap})^{l_j} \cdot (1 - p_j^{ion} - p_j^{cap})^{N_j - k_j - l_j}. \tag{28}$$

The sum $k + l$ is equal to the degree of electron removal from the target. Strictly speaking, equation (26) is a particular case of equation (28).

The net ionization and capture probabilities can be calculated as

$$P_{net}^{ion}(\rho) = \sum_{q=1}^{N} q \sum_{l=0}^{N-q} P_{q,l}^{tot}. \tag{39}$$

$$P_{net}^{cap}(\rho) = \sum_{q=1}^{N} q \sum_{k=0}^{N-q} P_{k,q}^{tot}, \tag{30}$$

where N is the number of target electrons.

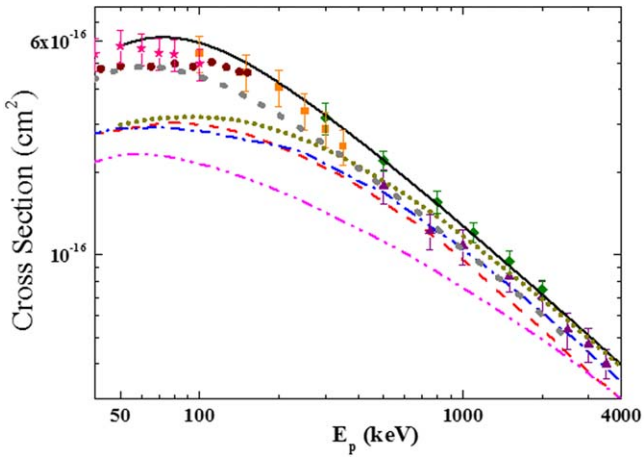

Figure 1. Cross sections for pure SI of H_2O by proton impact. Theories: solid line, 3B-CDW-EIS; short-dotted line, binomial 3B-CDW-EIS; dashed line, BGM from [18]; dash-dotted line, CDW-EIS-MO from [17]; dash-dot-dotted line, independent particle model CTMC from [22]; dotted line, independent event model CTMC from [22]. Experiments: (■), from [42]; (●), from [43]; (▲) and (∗), from [44]; (◆), from [10].

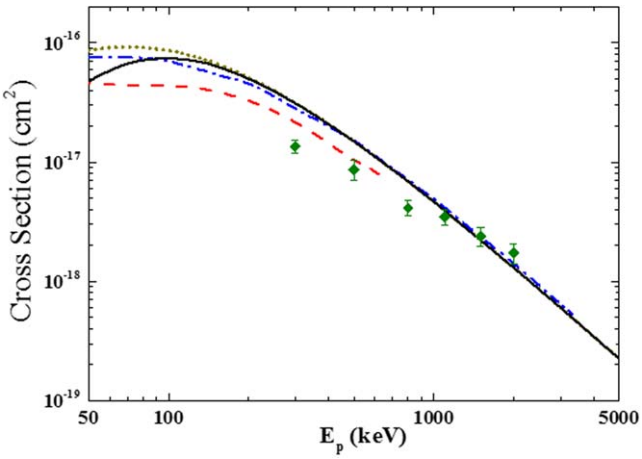

Figure 2. Cross sections for DI of H_2O by proton impact. Theories: solid line, 3B-CDW-EIS; dotted line, binomial 3B-CDW-EIS; dashed line, BGM from [18]; dash-dotted line, CDW-EIS-MO from [17]. Experiment: (◆), from [10].

3. Results and discussion

Applying our model to the proton−H_2O-vapor collision system, we have obtained single- and multiple-electron removal cross sections. After the calculation of single-particle probabilities $p^{ion}(\rho)$ and $p^{cap}(\rho)$, we found that they can exceed unity for sufficiently low impact energies and small impact parameters. To solve this problem we used the unitarization procedure suggested by Sidorovich [37] for each jth MO:

$$\hat{p}_j^{\alpha}(\rho) = \frac{p_j^{\alpha}(\rho)}{[p_j^{ion}(\rho) + p_j^{cap}(\rho)]} \times \{1 - \exp[-(p_j^{ion}(\rho) + p_j^{cap}(\rho))]\}, \quad (31)$$

where the index α can be taken as *ion* or *cap*. As previously indicated, its application is supported by its success in describing multiple-electron ionization DDCSs for highly-charged ions impacting on Ar and Ne atoms [38].

3.1. Single and multiple ionization

In figure 1 pure (exclusive) SI cross sections corresponding to different models in comparison with experimental data [10, 42–44] are shown.

The important point in our model is that we reduce the many-electron system to one active electron, while the remaining target electrons are frozen during the collision. It should be mentioned that TCSs from [42] and [44] were measured as SI + TI_{11} (TI_{11} is a simultaneous ionization of one electron and capture of one electron) cross sections. In [10], the measured production yields were corrected in order to obtain the true single-ion and ion-pair production yields. However, their result for SI is contaminated by the $H^+ + H^+ + O^0$ channel, because the detector was not able to distinguish between one and two H^+ ions coming from the same collision event. In the experiment corresponding to [44] these type of correction were not considered.

At impact energies larger than 300 keV good agreement with the experimental data of [10] is found. Previous BGM [18], CDW-EIS-MO [17], independent particle model CTMC (IPM-CTMC) [22] and independent event model CTMC (IEVM-CTMC) [22] calculations are also displayed in figure 1. The results of the BGM [18] and CDW-EIS-MO [17] calculations are in close agreement. However, both models underestimate the experimental data at low and intermediate energies. Moreover, the BGM tends to underestimate the experiments as the impact energy increases. As previously demonstrated, the reduction of the multielectron problem to a one-active-electron problem is obtained assuming that the passive electrons remain frozen in their initial orbitals [25], so that SI probabilities are consequently exclusive. Thus, a multinomial distribution statistical model, in particular a binomial one, should not be applied to study pure single-electron reactions. The binomial statistics are computed from equation (26) by setting $p^{cap}(\rho) = 0$.

The IPM interpretation in the framework of the CTMC model of [22] largely underestimates the experiments over all the energy range. However, the IEVM-CTMC approximation is in reasonable agreement with the measurements at low energies, but underestimates the data measured in [10] at higher energies.

Pure double electron ionization (DI) cross sections corresponding to different models and experimental data are plotted in figure 2.

The experimental data points in figure 2 result from the sum of two fragments of DI (the $H^+ + OH^+$ and $H^+ + O^+$ channels) obtained in [10]. Therefore, in order to evaluate the DI cross section, it is necessary to sum the contribution of the $H^+ + H^+ + O^0$ channel and subtract contamination of the $H^+ + O^+$ channel from the $H^+ + H^+ + O^+$ channel. However, at present, it is impossible to achieve this using the experimental setup described in [10]. The fragment $H^0 + H^0 + O^{2+}$ can be created from a H_2O^{2+} ion, but it has

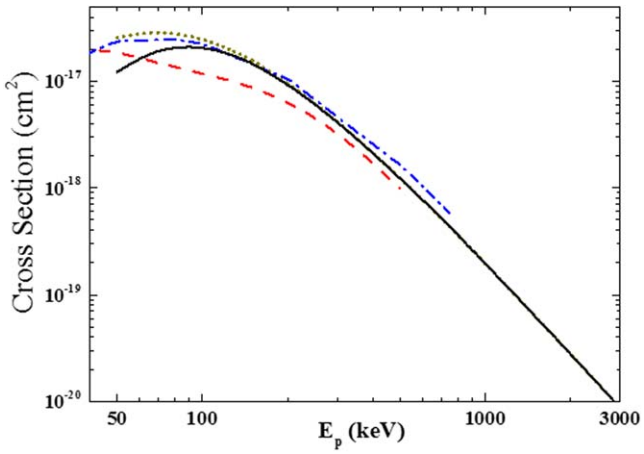

Figure 3. Cross sections for the TI of H_2O by proton impact. Theories: solid line, 3B-CDW-EIS; dotted line, binomial 3B-CDW-EIS; dashed line, BGM from [18]; dash-dotted line, CDW-EIS-MO from [17].

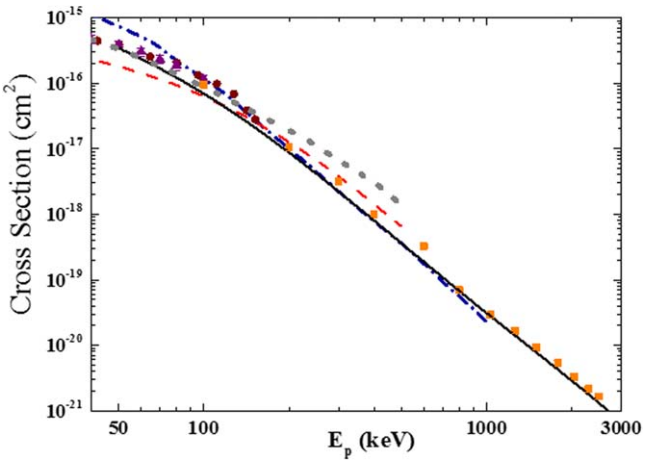

Figure 4. Cross sections for pure SC of H_2O by proton impact. Theories: solid line, 3B-CDW-EIS; dashed line, BGM [18]; short-dash-dotted line, CTMC from [20]; dotted line, IEVM-CTMC from [21]. Experiments: (■), from [39]; (●), from [43]; (▲), from [44].

been shown that it gives a minor contribution to the full DI [42, 43].

The 3B-CDW-EIS model shows good agreement with the experiment in [10] at high enough impact velocities and is in close agreement with the CDW-EIS-MO results. However, the 3B-CDW-EIS model overestimates the measurements at energies lower that 1 MeV. This should be attributed to the necessity of considering the interaction between the two ionized electrons in the exit channel. At these energies, the BGM results, also shown in the figure, give a better representation of the experiments.

We compare theoretical results for the pure triple ionization (TI) process in figure 3.

A close agreement of 3B-CDW-EIS with CDW-EIS-MO results is found, even considering that we have used a trinomial distribution for probabilities instead of the binomial one employed in the CDW-EIS-MO calculations [17]. The difference between both models at impact energies lower than 100 keV may be again partially attributed to the influence of capture reactions. In general, the BGM results underestimate both CDW-EIS approximations.

In order to estimate the influence of electron capture in the DI and TI reactions, calculations using a 3B-CDW-EIS binomial distribution (where charge exchange is neglected in the determination of ionization probabilities; see equation (26)) are included in figures 2 and 3. For both reactions, electron capture is found to contribute only at enough low impact velocities.

3.2. SC and transfer-ionization

Now, we turn our attention to the electron capture processes. Pure SC TCS results corresponding to different models are depicted in figure 4 along with available measurements [39, 43, 44].

Here we observe that the present model shows good general agreement with the measurements in [39], where the total SC was measured. Pure SC and transfer-ionization processes are included in the data of [43] and [44], which could explain the underestimation of experimental results by 3B-CDW-EIS at the lower energies, considering that the present calculations correspond to pure SC.

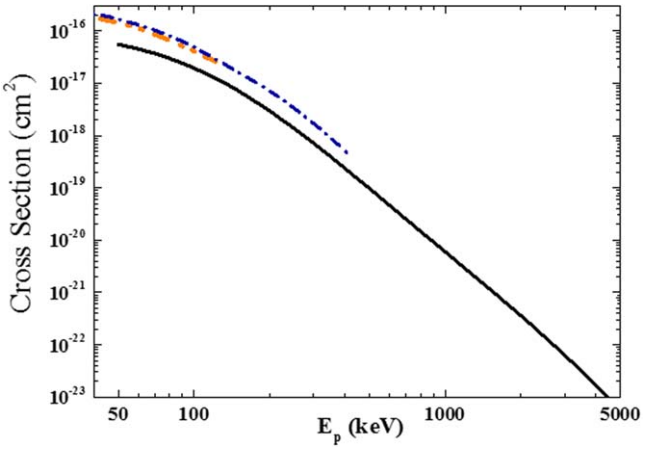

Figure 5. Cross sections for pure transfer-ionization TI_{11} of H_2O by proton impact. Theories: solid line, 3B-CDW-EIS; dash-dot-dotted line, IMP-CTMC from [19]; short-dash-dotted line, CTMC from [20].

SC TCSs computed employing BGM [18] are also included in the figure. They underestimate both our results and the experimental data at low impact energies, and slightly overestimate at intermediate to high energies. The CTMC approximation of [20] gives results in close accordance with the 3B-CDW-EIS results at the high energy range, but overestimates the existing measurements at low impact velocities. The IEVM-CTMC approximation [21] shows good agreement with experiments at low energies, but appears to overestimate them at higher energies.

To our knowledge, no pure transfer-ionization experimental data exist for the proton−H_2O-molecule collision system. Therefore, we compare our TI_{11} result with other theories in figure 5. Calculations corresponding to the two CTMC calculations [19, 20] are shown in figure 5. They are

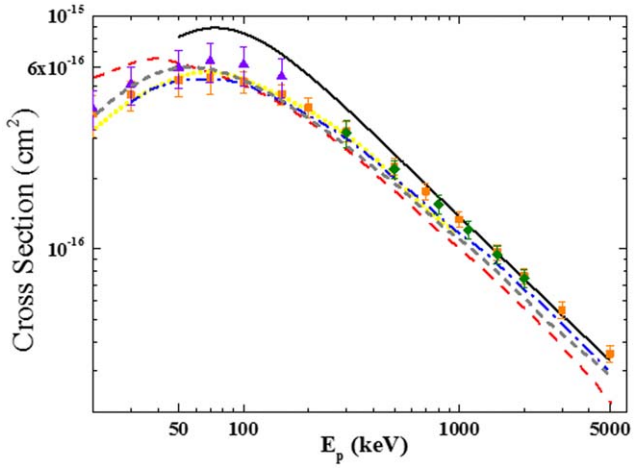

Figure 6. Net ionization cross sections of H_2O by proton impact. Theories: solid line, 3B-CDW-EIS; dashed line, BGM from [18]; dash-dotted line, CDW-EIS-MO from [17]; short-dotted line, PCM-BGM from [47]; short-dashed line, IEVM-CTMC from [22]. Experiments: (■), from [40]; (▲), from [41]; (◆), from [10].

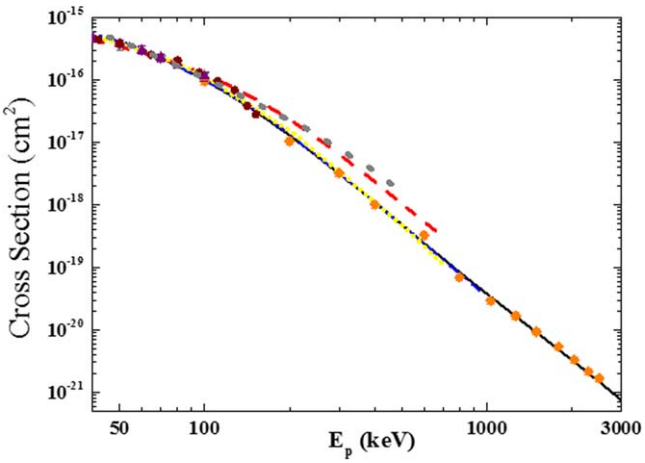

Figure 7. Net capture cross sections of H_2O by proton impact. Theories: solid line, 3B-CDW-EIS; dashed line, BGM from [18]; dash-dotted line, CDW-EIS-MO from [17]; short-dotted line, PCM-BGM from [47]; dotted line, IEVM-CTMC from [21]. Experiments: (◆), from [39]; (▼) from [40]; (●), from [43]; (▲), from [44].

almost identical, giving cross sections larger than the present 3B-CDW-EIS model.

3.3. Net ionization and capture

The net ionization cross sections are displayed in figure 6 as a function of the impact energy. They are calculated using the expression:

$$\sigma_{net}^{ion} = \sigma_{SI} + 2\sigma_{DI} + 3\sigma_{TI} + \sigma_{TI_{11}} + 2\sigma_{TI_{21}}. \tag{32}$$

The data from [10] for pure SI are included in figure 6, because SI is a key channel in the net ionization for high energies. It is found that 3B-CDW-EIS presents good agreement with measurements at high energies and tends to overestimate them at energies lower than 500 keV. On the other hand, we observed in figure 1 that 3B-CDW-EIS gives a good representation of experiments for pure SI. It should be noted that, to our knowledge, there are no experimental data for pure σ_{TI}, $\sigma_{TI_{11}}$, $\sigma_{TI_{21}}$ ($\sigma_{TI_{21}}$ is a transfer-ionization cross section with simultaneous ionization of two electrons and capture of one electron) and there exist only a scarce number of measured points for pure σ_{DI}.

The BGM model [18] underestimates measurements at high impact energies and the maximum of their curve is shifted to low energies. A new pixel counting method in the framework of BGM (PCM-BGM) [47] and the IEVM-CTMC model [22] show good agreement with the experiments at low and intermediate impact energies, but tend to underestimate them at higher energies. At the present stage of PCM-BGM [47], it can be used only for calculation of the net ionization or net capture cross sections. The results of the CDW-EIS-MO model [17] give a good description of experiments at low and intermediate range, but slightly underestimate them at high energies. In fact, to perform a complete analysis of the net ionization cross sections it appears to be necessary to give an appropriate description of each contributing individual reaction.

Net electron capture cross sections for the $H^+ - H_2O$ collision system, which are plotted in figure 7, are calculated using the expression:

$$\sigma_{net}^{cap} = \sigma_{SC} + \sigma_{TI_{11}} + \sigma_{TI_{21}}. \tag{33}$$

In the experiment presented in [40], measured SCs are obtained as

$$\sigma_c = \sigma_+ - \sigma_-, \tag{34}$$

where σ_+ is the total target positive-charge production cross section and σ_- is the total target-electron production cross section. This means that their results might include all single and multiple capture and transfer-ionization cross sections.

TCSs calculated within the 3B-CDW-EIS approximation are in excellent agreement with experiments [39, 40, 43, 44]. The results of BGM [18] and IEVM-CTMC [21] give a good description of measurements at low energies, but overestimate them at larger impact velocities. It would be interesting to explore if this overestimation in the BGM framework [18] (as well as the underestimation with respect to other theoretical TCS predictions for electron ionization) is caused by the use of the sinusoidal ansatz based on only two fixed molecular orientations to average over all molecular orientations. The curves corresponding to the PCM-BGM [47] and CDW-EIS-MO [17] approximations are very close to the 3B-CDW-EIS results. However, as was mentioned above, the PCM-BGM method [47] gives just appropriate net cross sections and in the framework of the CDW-EIS-MO approximation [17] transfer-ionization processes were not included, which could give a non-negligible contribution at intermediate to low projectile energies. Finally, we must remark that, as has been indicated for net ionization, TCSs for net electron capture can give only an average result without information about each pure process.

4. Conclusions

Single- and multiple-electron removal processes of water-vapor targets impacted by protons were investigated within the first-order of the 3B-CDW-EIS perturbative series. The model is based on the reduction of the multielectron dynamical system to a single-active-electron one. In order to obtain this reduction the residual electrons are considered to remain frozen in their initial states during the collision. Then, single-electron ionization and single-electron capture probabilities are determined. These single-electron processes are calculated separately from a defined initial state to a defined final one, without the necessity of additional approximations. It is shown that the model gives an adequate description of pure single-electron reactions.

In order to investigate multiple-electron processes, a statistical trinomial distribution is employed. This has been shown to give a generally appropriate representation of the corresponding existing experimental data for net cross sections. However, it is also proven that the multinomial analysis cannot be satisfactorily applied for pure single-electron processes. We must remark that net electron ionization and net electron capture TCSs result from the sum of separate contributions coming from pure reactions. Therefore, new measurements for pure multiple-electron processes would be welcome for a more complete description of the different reactions and to avoid possible compensation of individual contributions when net cross sections are determined.

The developed approach can also be used to investigate water fragmentation mechanisms and allow us to build models including Auger-type post-collisional effects, which are expected to give important contributions at high projectile impact energies when multiple-electron removal processes occur (see [48, 49] for atomic targets). In [48, 49] it is shown that the inclusion of post-collisional effects improves the theoretical agreement with available experimental data, particularly in the high impact energy region, and for high q-order ionization. At the present time, we are working on the inclusion of post-collisional effects in the case of molecular targets, for both q-order ionization and capture. Future work will also be focused on evaluating single- and multiple-electron removal cross sections for highly-charged projectiles (He^{2+}, Li^{3+}, C^{6+}) colliding with water and DNA/RNA macromolecules for possible applications in ion beam therapy. With such a goal in mind, we plan to use the Sidorovich normalization method which, as mentioned earlier, has been applied with success to describe multiple-ionization DDCSs of atomic targets by interaction with highly-charged ions.

Acknowledgments

The authors acknowledge financial support from the Agencia Nacional de Promoción Científica y Tecnológica (PICT's No. 2011-1912 and 2015-3392) and from the Consejo Nacional de Investigaciones Científicas y Técnicas de la República Argentina (PIP No. 0784). This work has been carried out using the computing resources of the Instituto de Física Rosario and the federal collective usage center, the Complex for Simulation and Data Processing for Mega-science Facilities at NRC 'Kurchatov Institute' (ministry subvention under agreement RFMEFI62117X0016), http://ckp.nrcki.ru/. The contributions of both institutions are acknowledged. RDR also acknowledges the hospitality of the Bar Vittorio in Rosario, where part of this work was written.

ORCID iDs

P N Terekhin https://orcid.org/0000-0002-6616-7351
M A Quinto https://orcid.org/0000-0002-1598-9128

References

[1] Murakami I, Yan J, Sato H, Kimura M, Janev R K and Kato T 2008 *At. Data Nucl. Data Tables* **94** 161
[2] Yu S S *et al* 2007 *Nucl. Fusion* **47** 721
[3] Brahme A 2004 *Int. J. Radiat. Oncol. Biol. Phys.* **58** 603
[4] Heinrichs A 2009 *Nat. Rev. Mol. Cell Biol.* **10** 239
[5] Nikjoo H and Lindborg L 2010 *Phys. Med. Biol.* **55** R65
[6] Yokoya A, Shikazono N, Fujii K, Urushibara A, Akamatsu K and Watanabe R 2008 *Radiat. Phys. Chem.* **77** 1280
[7] Rudd M E 1989 *Int. J. Radiat. Appl. Instrum.* D **16** 213
[8] Hansen J P and Kocbach L 1989 *J. Phys. B: At. Mol. Opt. Phys.* **22** L71
[9] Bernal M A and Liendo J A 2007 *Nucl. Instrum. Methods Phys. Res.* B **262** 1
[10] Tavares A C, Luna H, Wolff W and Montenegro E C 2015 *Phys. Rev.* A **92** 032714
[11] Boudrioua O, Champion C, Dal Cappello C and Popov Y V 2007 *Phys. Rev.* A **75** 022720
[12] Dal Cappello C, Champion C, Boudrioua O, Lekadir H, Sato Y and Ohsawa D 2009 *Nucl. Instrum. Methods Phys. Res.* B **267** 781
[13] Champion C and Dal Cappello C 2009 *Nucl. Instrum. Methods Phys. Res.* B **267** 881
[14] Houamer S, Popov Y V, Dal Cappello C and Champion C 2009 *Nucl. Instrum. Methods Phys. Res.* B **267** 802
[15] Olivera G H, Fainstein P D and Rivarola R D 1996 *Phys. Med. Biol.* **41** 1633
[16] Tachino C A, Monti J M, Fojón O A, Champion C and Rivarola R D 2014 *J. Phys. B: At. Mol. Opt. Phys.* **47** 035203
[17] Gulyás L, Egri S, Ghavaminia H and Igarashi A 2016 *Phys. Rev.* A **93** 032704
[18] Murakami M, Kirchner T, Horbatsch M and Lüdde H J 2012 *Phys. Rev.* A **85** 052704
[19] Errea L F, Illescas C, Méndez L, Pons B, Rabadán I and Riera A 2007 *Phys. Rev.* A **76** 040701(R)
[20] Lekadir H, Abbas I, Champion C and Hanssen J 2009 *Nucl. Instrum. Methods Phys. Res.* B **267** 1011
[21] Illescas C, Errea L F, Méndez L, Pons B, Rabadán I and Riera A 2011 *Phys. Rev.* A **83** 052704
[22] Errea L F, Illescas C, Méndez L and Rabadán I 2013 *Phys. Rev.* A **87** 032709
[23] Lüdde H J, Spranger T, Horbatsch M and Kirchner T 2009 *Phys. Rev.* A **80** 060702(R)
[24] Hehre W J, Stewart R F and Pople J A 1969 *J. Chem. Phys.* **51** 2657
[25] Fainstein P D, Ponce V H and Rivarola R D 1988 *J. Phys. B: At. Mol. Opt. Phys.* **21** 287

[26] Rivarola R D, Piacentini R D, Salin A and Belkić Dž 1980 *J. Phys. B: At. Mol. Opt. Phys.* **13** 2601
[27] Monti J M, Fojón O A, Hanssen J and Rivarola R D 2013 *J. Phys. B: At. Mol. Opt. Phys.* **46** 145201
[28] Monti J M, Tachino C A, Hanssen J, Fojón O A, Galassi M E, Champion C and Rivarola R D 2014 *Appl. Radiat. Isot.* **83** 105
[29] Quinto M A, Montenegro P R, Monti J M, Fojón O A and Rivarola R D 2018 *J. Phys. B: At. Mol. Opt. Phys.* **51** 165201
[30] Pople J A, Santry D P and Segal G A 1965 *J. Chem. Phys.* **43** S129
[31] Clementi E and Roetti C 1974 *At. Data Nucl. Data Tables* **14** 177
[32] Moccia R 1964 *J. Chem. Phys.* **40** 2186
[33] Stolterfoht N, DuBois R D and Rivarola R D 1997 *Electron Emission in Heavy Ion–Atom Collisions* (*Springer Series on Atomic, Optical and Plasma Physics*) vol 20 (Berlin: Springer)
[34] Stephen B J, Pople John A and Hehre Warren J 1980 *J. Am. Chem. Soc.* **102** 939
[35] Nandi S, Biswas S, Khan A, Monti J M, Tachino C A, Rivarola R D, Misra D and Tribedi L C 2013 *Phys. Rev.* A **87** 052710
[36] Bhattacharjee S *et al* 2016 *J. Phys. B: At. Mol. Opt. Phys.* **49** 065202
[37] Sidorovich V A and Nikolaev V S 1983 *J. Phys. B: At. Mol. Opt. Phys.* **16** 3243
[38] Kirchner T, Gulyás L, Moshammer R, Schulz M and Ullrich J 2002 *Phys. Rev.* A **65** 042727
[39] Toburen L H, Nakai M Y and Langley R A 1968 *Phys. Rev.* **171** 114
[40] Rudd M E, Goffe T V, DuBois R D and Toburen L H 1985 *Phys. Rev.* A **31** 492
[41] Bolorizadeh M A and Rudd M E 1986 *Phys. Rev.* A **33** 888
[42] Werner U, Beckord K, Becker J and Lutz H O 1995 *Phys. Rev. Lett.* **74** 1962
[43] Gobet F *et al* 2006 *Phys. Rev.* A **70** 062716
[44] Luna H *et al* 2007 *Phys. Rev.* A **75** 042711
[45] Belkić D, Gayet R and Salin A 1979 *Phys. Rep.* **56** 279
[46] Horbatsch M 1994 *Phys. Lett.* A **187** 185
[47] Lüdde H J, Achenbach A, Kalkbrenner T, Jankowiak H-C and Kirchner T 2016 *Eur. Phys. J.* D **70** 82
[48] Galassi M E, Rivarola R D and Fainstein P D 2007 *Phys. Rev.* A **75** 052708
[49] Tachino C A, Galassi M E and Rivarola R D 2008 *Phys. Rev.* A **77** 032714